

# Difference in the Reactivities of H- and Me-Substituted Dinucleating Bis(iminopyridine) Ligands with Nickel(0)

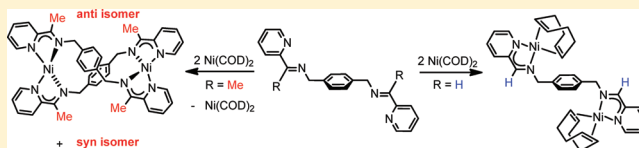
Amarnath Bheemaraju,<sup>†</sup> Richard L. Lord,<sup>†</sup> Peter Müller,<sup>‡</sup> and Stanislav Groysman<sup>\*,†</sup>

<sup>†</sup>Department of Chemistry, Wayne State University, Detroit, Michigan 48202, United States.

<sup>‡</sup>Department of Chemistry, Massachusetts Institute of Technology, Cambridge, Massachusetts 02139, United States

## S Supporting Information

**ABSTRACT:** The reactivity of dinucleating bis(iminopyridine) ligands bearing H ( $L^1$ , ( $N,N'$ )-1,1'-(1,4-phenylene)bis( $N$ -(pyridin-2-ylmethylene)methanamine)) or Me substituents ( $L^2$ , ( $N,N'$ )-1,1'-(1,4-phenylene)bis( $N$ -(1-(pyridin-2-yl)ethylidene)methanamine)) on the imine carbon atom with  $Ni(COD)_2$  (COD = 1,5-cyclooctadiene) has been investigated. Treatment of  $L^1$  with 2 equiv of  $Ni(COD)_2$  forms dinuclear  $Ni_2(L^1)(COD)_2$ , whereas the reaction of  $L^2$  with 2 equiv of  $Ni(COD)_2$  leads to  $Ni_2(L^2)_2$ , along with 1 equiv of  $Ni(COD)_2$ . The compounds were characterized by  $^1H$  and  $^{13}C$  NMR spectroscopy, mass spectrometry, and elemental analysis; the structure of  $Ni_2(L^2)_2$  was determined by XRD.  $Ni_2(L^2)_2$  exists as syn and anti stereoisomers in the solid state and in solution. DFT calculations suggest Ni(I) for both  $Ni_2(L^1)(COD)_2$  and  $Ni_2(L^2)_2$ , with the radical anion localized on one iminopyridine fragment in  $Ni_2(L^1)(COD)_2$  and delocalized over two iminopyridine fragments in  $Ni_2(L^2)_2$ . Both  $Ni_2(L^1)(COD)_2$  and  $Ni_2(L^2)_2$  undergo a reaction with excess diphenylacetylene, forming diphenylacetylene complexes. However, whereas  $Ni_2(L^1)(diphenylacetylene)_2$  decomposes upon removal of the excess diphenylacetylene,  $Ni_2(L^2)_2$  demonstrates a reversible disassembly/reassembly sequence upon the addition/removal of diphenylacetylene.



Redox-noninnocent<sup>1</sup> ligands play an active role in redox transformations mediated by a metal–ligand system.<sup>2</sup> Delineation of the factors that control the reactivity of the redox-active ligand systems is important for their application in catalysis.<sup>3</sup> Iminopyridines have been recently demonstrated to possess noninnocent ligand character,<sup>4,5</sup> closely related to that of the much studied  $\alpha$ -diimines,<sup>6</sup> bis(imino)pyridines,<sup>7</sup> and bipyridines.<sup>8</sup> The majority of the iminopyridine systems investigated so far had an H substituent on the imine carbon atom.<sup>4,5,9–12</sup> Herein, we demonstrate that the nature of the substituent can have a profound impact on the reactivity of these ligands with reduced metal centers.

We are targeting dinucleating redox-active ligand platforms for cooperative dinuclear and multinuclear catalysis. As our first goal, we aim to develop the chemistry of the dinucleating bis(iminopyridine) ligands, depicted in Figure 1, that are capable of binding reduced metal centers. As part of the ligand design, we decided to investigate two different substituents attached to the imine carbon atom: H ( $L^1$ ) and Me ( $L^2$ ).  $L^1$  and

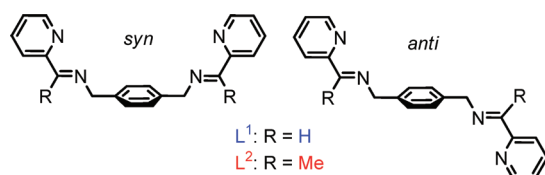


**Figure 1.** Syn and anti conformations of the bis(iminopyridine) ligands  $L^1$  and  $L^2$ .

$L^2$  are flexible ligands, enabling syn and anti relative orientations of the iminopyridine chelating units.  $L^1$  has been previously shown to form both dinuclear complexes<sup>13</sup> and metallosupramolecular systems,<sup>14</sup> depending on the reaction conditions;  $L^2$  has not been synthesized before.  $L^1$  and  $L^2$  were obtained by condensation of 1,4-xylylenediamine with carboxypyridine ( $L^1$ ) or acetylpyridine ( $L^2$ ) and were isolated as crystalline solids from MeOH, in 81% ( $L^1$ ) and 76% ( $L^2$ ) yields.

Next, we targeted dinuclear Ni species. Treatment of 2 equiv of  $Ni(COD)_2$  with  $L^1$  forms blue-violet **1a**, isolated in 57% yield (Figure 2). The  $^1H$  NMR spectrum of **1a** is consistent with the expected  $Ni_2(L^1)(COD)_2$  formulation. Most characteristically, COD signals are observed at 3.8, 2.7, and 1.7 ppm, supporting its rigid binding to the metal<sup>6g,k,15</sup> (Figure S5, Supporting Information). Furthermore, the asymmetric nature of the iminopyridine ligand leads to two sets of signals for the alkene CH (around 3.8 ppm) and for one of the methylene (2.7 ppm) protons. The  $^{13}C$  NMR is consistent with these observations (Figure S6), displaying two sets of CH (82.8 and 81.9 ppm) and  $CH_2$  (31.4, 31.3 ppm) signals. The methylene ( $NCH_2Ph$ ) protons of the ligand backbone appear as a sharp singlet (5.26 ppm), consistent with a flexible behavior of **1a**. Further support for the formation of **1a** was obtained by mass spectrometry. The compound displays limited stability under vacuum or in solution for prolonged

Received: January 26, 2012

Published: March 8, 2012

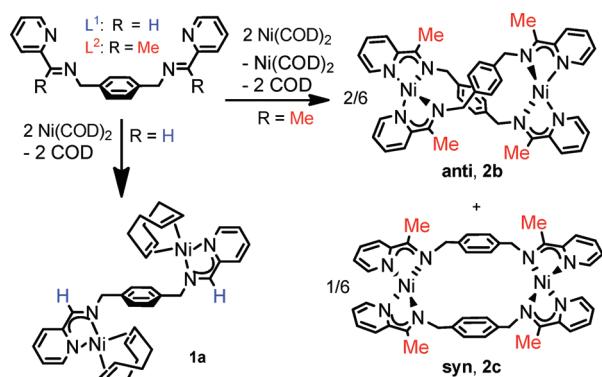


Figure 2. Reactivity of  $L^1$  and  $L^2$  with  $Ni(COD)_2$ .

periods of time, forming an insoluble brown material. As a result, our multiple attempts to obtain its crystal structure proved unsuccessful.

The reaction of  $L^2$  with 2 equiv of  $Ni(COD)_2$  took a different path. Under identical reaction conditions, purple product **2** was formed, along with an equimolar amount of  $Ni(COD)_2$ . The  $^1H$  NMR spectrum of **2** in  $C_6D_6$  at room temperature exhibits two sets of resonances attributable to two different species (**2b,c**) in a ca. 2:1 ratio and no signals attributable to COD (Figure S7). The imino Me groups gave rise to two peaks at  $-0.3$  and  $-0.5$  ppm. This unusual chemical shift for a Me group is consistent with a Me group in the vicinity of a radical anion,<sup>7b</sup> indicating noninnocent behavior of  $L^2$  upon coordination to the reduced Ni centers. The presence of two different structural isomers (**2b,c**) was confirmed by an X-ray structure determination (Figure 3). Two isomers are present in the asymmetric unit in a 2:1 ratio (nearly identical with the NMR ratio). The prevalent isomer, **2b**, features an anti conformation of the chelating iminopyridine units in  $L^2$ , whereas **2c** has a syn conformation of the iminopyridine units.  $L^1$  has been reported to feature either syn<sup>14b</sup> or a mixture of syn and anti isomers<sup>14a</sup> in supramolecular assemblies. Different isomers have been proposed to be stabilized by noncovalent packing interactions.<sup>14</sup> Herein, we show that discrete, molecular species can display similar isomerism both in solution ( $^1H$  NMR) and in the solid state. The average imine C–C (1.43 Å) and C–N (1.33 Å) bonds are similar between the structures and are intermediate between those of singly reduced (1.41 Å and 1.34 Å) and neutral (1.47 Å and 1.28 Å) iminopyridine.<sup>4a</sup> Dihedral angles between Ni–N–N planes are similar for the anti (**2b**) and syn (**2c**) structures ( $51^\circ$ ). We note that a dinucleating bis(iminopyridine) ligand with a shorter linker,  $N,N'$ -bis(6-methyl-2-pyridylmethylene)ethane-1,2-diamine, has been shown to form di-Ni complexes featuring the anti geometry exclusively.<sup>16</sup>

We monitored both transformations by  $^1H$  NMR spectroscopy in toluene- $d_8$  at  $23^\circ C$  (Supporting Information). For  $L^1$ , only reactants ( $L^1$  and  $Ni(COD)_2$ ) and products (**1a** and COD) are observed. The formation of **1a** is fast: it is almost complete within several minutes (Figure S22). No traces of the **1b** or **1c** dimer (see below) were detected during the time the reaction was monitored by  $^1H$  NMR (ca. 6 h). In contrast, the reaction of  $L^2$  with  $Ni(COD)_2$  is slow: signals of free  $L^2$  were present in the spectrum after ca. 2 h ( $\delta$  4.59 ppm, Figure S19). Furthermore, signals attributable to  $Ni_2(L^2)(COD)_2$  were observed in the reaction of  $L^2$  with 2 equiv of  $Ni(COD)_2$ . Initially,  $Ni_2(L^2)(COD)_2$  was observed as a predominant

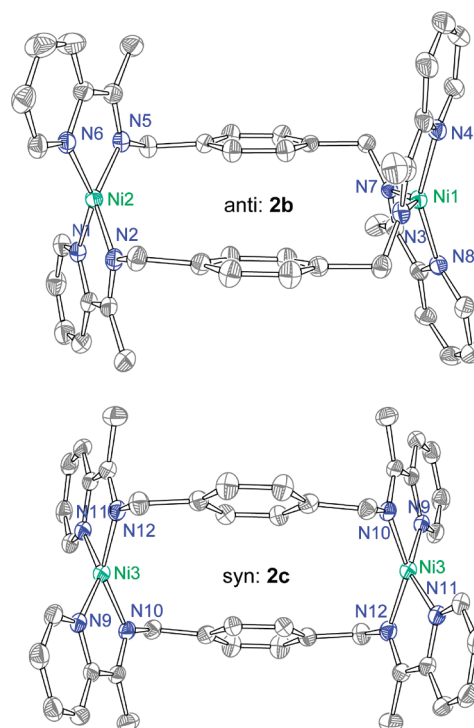
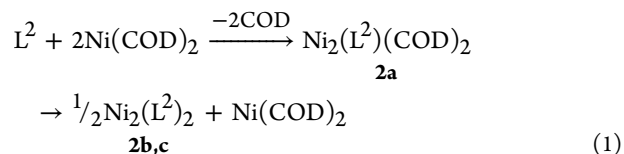


Figure 3. Solid-state structure of the anti (**2b**) and syn (**2c**) stereoisomers of **2** (50% probability ellipsoids). Hydrogen atoms and solvent molecules were omitted for clarity. The ratio of **2b** to **2c** in the structure is 2:1, as a full molecule of **2b** and a half-molecule of **2c** occupy an asymmetric unit.

product, but as the reaction progressed the concentration of  $Ni_2(L^2)(COD)_2$  decreased and the concentration of  $Ni_2(L^2)_2$  increased. After 5 h,  $Ni_2(L^2)(COD)_2$  constituted  $<10\%$  of  $Ni_2(L^2)_2$  in the reaction mixture. These concentration profiles suggest that  $Ni_2(L^2)(COD)_2$  is an intermediate in the formation of  $Ni_2(L^2)_2$ . (see eq 1).



Treatment of  $L^2$  with 1 equiv of  $Ni(COD)_2$  leads to the formation of **2b,c** in 63% isolated yield. The reaction of  $L^1$  with 1 equiv of  $Ni(COD)_2$  leads to the formation of the similar isomer mixture **1b,c** (98%). Different imine carbon substituents lead to a different distribution of the isomers. Whereas **2b,c** appear in a 2:1 ratio, the order is reversed for **1b,c**, displaying a 2:3 ratio.<sup>17</sup> The syn isomer is the major product for the **1b,c** mixture. To probe further the nature of complex isomerism in  $Ni^2(L^2)_2$  species in solution, we carried out variable-temperature NMR experiments in toluene- $d_8$ . The anti to syn ratio of isomers **2b,c** varies as a function of temperature: cooling to  $-80^\circ C$  further destabilizes **2c** (ratio 2/0.6), whereas heating the mixture to  $80^\circ C$  increases the proportion of **2c** in the mixture (ratio 2/1.3).

To get insight into the oxidation state distribution between the metal and the ligands, we performed density functional theory calculations on a model bis(iminopyridine) complex.<sup>18</sup> The lowest energy electronic state for  $[Ni(L^3)_2]^{0+}$  (see Figure 4 for ligand definition) is an antiferromagnetically (AF) coupled singlet species that we computed using the broken symmetry

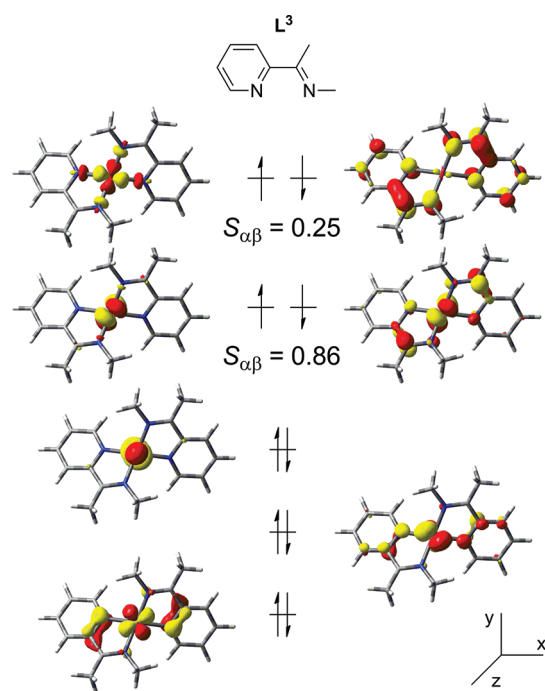


**Figure 4.** Top-down view of isodensity surfaces (0.05 au) for the  $[\text{Ni}(\text{L}^3)_2]^0$  corresponding orbitals.  $S_{\alpha\beta}$  is the overlap between the  $\alpha$  and  $\beta$  orbitals and is only listed for nonunity ( $<0.99$ ) values.

formalism.<sup>19,20</sup> Computed bond lengths of 1.44 and 1.33 Å for the imine C–C and C–N bonds agree well with those observed in the crystal structure. The corresponding orbital analysis for  $[\text{Ni}(\text{L}^3)_2]^0$  (Figure 4) shows a Ni  $d_{x^2-y^2}$  radical magnetically coupled to a ligand  $\pi$  radical with an overlap of 0.25, suggesting weak AF coupling.<sup>21</sup> A second orbital has nonunity overlap, though the value is large at 0.86 and both orbitals are dominated by  $d_\pi$  character. We therefore assign this as a doubly occupied Ni  $d_\pi$  orbital. A Mulliken spin density of 1.1 at Ni further supports assignment as  $\text{Ni}^{\text{I}}$ , though the data could be alternatively interpreted as having a fractional oxidation state between  $\text{Ni}^{\text{I}}$  and  $\text{Ni}^{\text{II}}$ . Wiegardt and co-workers observed similar behavior for a related bis(iminopyridine) complex.<sup>4a</sup> We also computed the electronic structure for a model of  $[\text{Ni}(\text{L}^1)(\text{COD})]^0$ . The results suggest a  $\text{Ni}^{\text{I}}$  center and a monoanionic iminopyridine ligand, in contrast to the case for the bis(iminopyridine) complex. Additional model complexes with different substituents on the imine carbon show that the electronic structure at Ni and iminopyridine does not qualitatively change for the two bis(iminopyridine) and iminopyridine–COD complexes as a function of the substituent. A full analysis of all species can be found in the Supporting Information.

Thus, we postulated that  $\text{L}^2$  in  $\text{Ni}_2(\text{L}^2)_2$  will be more labile than  $\text{L}^1$  in  $\text{Ni}_2(\text{L}^1)(\text{COD})_2$ . Our initial reactivity studies have focused on the reactions of  $\text{Ni}_2(\text{L}^1)(\text{COD})_2$  and  $\text{Ni}_2(\text{L}^2)_2$  with diphenylacetylene as a  $\pi$ -acid model. Treatment of  $\text{Ni}_2(\text{L}^1)(\text{COD})_2$  with excess diphenylacetylene (4 equiv) leads to the replacement of COD ligands, forming  $\text{Ni}_2(\text{L}^1)(\text{PhCCPh})_2$  (**3a**). However, removal of the excess diphenylacetylene leads to the formation of an insoluble brown material, precluding the isolation of **3a** in a pure form. As no free ligand was detected in the soluble phase, we propose that  $\text{L}^1$  remains coordinated to Ni, consistent with its stronger coordination to the metal. In contrast,  $\text{Ni}_2(\text{L}^2)_2$  displays reversible binding of diphenylacety-

lene (Figure 5). Treatment of **2b,c** with excess diphenylacetylene (4 equiv) opens the dimer  $\text{Ni}_2(\text{L}^2)_2$  to give a mixture of

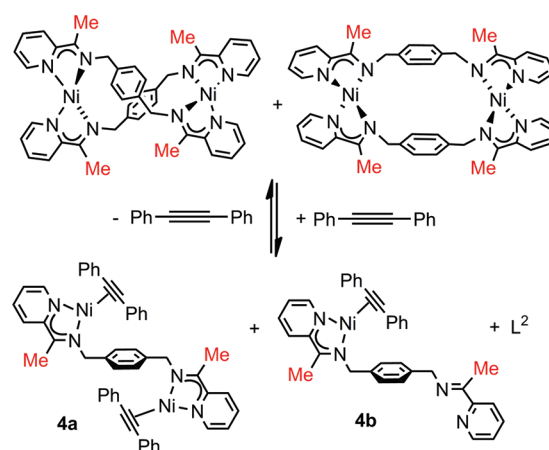


**Figure 5.** Reaction of  $\text{Ni}_2(\text{L}^2)_2$  with diphenylacetylene.

$\frac{1}{2} \text{Ni}_2(\text{L}^2)(\text{PhCCPh})_2$  (**4a**),  $\text{Ni}(\text{L}^2)(\text{PhCCPh})$  (**4b**), and  $\frac{1}{2} \text{L}^2$  (identified by NMR and mass spectrometry). Upon removal of excess diphenylacetylene with hexane, most of the material reverts back to the  $\text{Ni}_2(\text{L}^2)_2$  form. Thus,  $\text{Ni}^2(\text{L}^2)_2$  is an attractive candidate for the investigation of catalytic processes involving  $\pi$ -acids. It can break into monomers to bind the substrate and may reassemble into the stable resting state following the departure of the product.

To conclude, we have demonstrated a significant effect of the substituent on the imine carbon of the redox-active bis(iminopyridine) ligands on their reactivity with a  $\text{Ni}(0)$  precursor. For the H substituent, the dinuclear species  $\text{Ni}_2(\text{L}^1)(\text{COD})_2$  is formed, whereas the Me substituent leads to the formation of dinuclear  $\text{Ni}_2(\text{L}^2)_2$ .  $\text{Ni}_2(\text{L}^1)_2$  can be obtained by the reaction of 1 equiv of  $\text{L}^1$  with  $\text{Ni}(\text{COD})_2$ .  $\text{Ni}_2(\text{L}^1)_2$  and  $\text{Ni}_2(\text{L}^2)_2$  exist as a mixture of stereoisomers featuring syn and anti dispositions of the iminopyridine chelating units. The syn/anti ratio of the isomers is controlled by the imine carbon substituent and by temperature. DFT calculations suggest  $\text{Ni}(\text{I})$  as the oxidation state in both **1a** and **2b,c**. Delocalization of the radical anion over the two iminopyridine units in  $\text{Ni}_2(\text{L}^2)_2$  species is consistent with a labile coordination of  $\text{L}^2$  that enables  $\text{L}^2$  substitution by diphenylacetylene. We are continuing investigation of the reactivity of the reported complexes.

## ■ ASSOCIATED CONTENT

### Supporting Information

Text, figures, tables, and a CIF file giving full experimental procedures, NMR spectra, computational details and calculated structures, and X-ray data. This material is available free of charge via the Internet at <http://pubs.acs.org>.

## ■ AUTHOR INFORMATION

### Corresponding Author

\*E-mail: [groysman@chem.wayne.edu](mailto:groysman@chem.wayne.edu).

### Notes

The authors declare no competing financial interest.



## ACKNOWLEDGMENTS

We thank Wayne State University for funding. S.G. thanks Prof. D. G. Nocera and Prof. H. B. Schlegel for helpful discussions. A.B. thanks Bashar Ksebati and Lew Hryhorczuk for experimental assistance.

## REFERENCES

- (1) Caulton, K. G. *Eur. J. Inorg. Chem.* **2012**, 3, 435–443.
- (2) Chirik, P. J.; Wieghardt, K. *Science* **2010**, 327, 794–795.
- (3) For a recent thematic forum on redox non-innocent ligands see: *Inorg. Chem.* **2011**, 50, 9737–9914.
- (4) (a) Lu, C. C.; Bill, E.; Weyhermüller, T.; Bothe, E.; Wieghardt, K. *J. Am. Chem. Soc.* **2008**, 130, 3181–3197. (b) Van Gestel, M.; Lu, C. C.; Wieghardt, K.; Lubitz, W. *Inorg. Chem.* **2009**, 48, 2626–2632. (c) Lu, C. C.; Weyhermüller, T.; Bill, E.; Wieghardt, K. *Inorg. Chem.* **2009**, 48, 6055–6064.
- (5) (a) Myers, T. W.; Berben, L. A. *J. Am. Chem. Soc.* **2011**, 133, 11865–11867. (b) Myers, T. W.; Kazem, N.; Stoll, S.; Britt, R. D.; Shanmugam, M.; Berben, L. A. *J. Am. Chem. Soc.* **2011**, 133, 8662–8672.
- (6) For selected examples, see: (a) Balch, A. L.; Holm, R. H. *J. Am. Chem. Soc.* **1966**, 88, 5201–5209. (b) Gagnè, R. R.; Ingle, D. M.; Lisensky, G. C. *Inorg. Chem.* **1981**, 20, 1991–1993. (c) Hannant, M. D.; Schormann, M.; Bochmann, M. *Dalton Trans.* **2002**, 4071–4073. (d) Bart, S. C.; Hawrelak, E. J.; Schmisser, A. K.; Lobkovsky, E.; Chirik, P. J. *Organometallics* **2004**, 23, 237–246. (e) Bart, S. C.; Hawrelak, E. J.; Lobkovsky, E.; Chirik, P. J. *Organometallics* **2005**, 24, 5518–5527. (f) Chlopek, K.; Bothe, E.; Neese, F.; Weyhermüller, T.; Wieghardt, K. *Inorg. Chem.* **2006**, 45, 6298–6307. (g) Schaub, T.; Radius, U. Z. *Anorg. Allg. Chem.* **2006**, 632, 807–813. (h) Muresan, N.; Lu, C. C.; Ghosh, M.; Peters, J. C.; Abe, M.; Henling, L. M.; Weyhermüller, T.; Bill, E.; Wieghardt, K. *Inorg. Chem.* **2008**, 47, 4579–4590. (i) Ghosh, M.; Weyhermüller, T.; Wieghardt, K. *Dalton Trans.* **2008**, 5149–5151. (j) Liu, Y.; Li, S.; Yang, X.-J.; Yang, P.; Gao, J.; Xia, Y.; Wu, B. *Organometallics* **2009**, 28, 5270–5272. (k) Sgro, M. J.; Stephan, D. W. *Dalton Trans.* **2010**, 39, 5786–5796. (l) Knisley, T. J.; Saly, M. J.; Heeg, M. J.; Roberts, J. L.; Winter, C. H. *Organometallics* **2011**, 30, 5010–5017. (m) Kraft, S. J.; Williams, U. J.; Daly, S. R.; Schelter, E. J.; Kozimor, S. A.; Boland, K. S.; Kikkawa, J. M.; Forrest, W. P.; Christensen, C. N.; Schwarz, D. E.; Fanwick, P. E.; Clark, D. L.; Conradson, S. D.; Bart, S. C. *Inorg. Chem.* **2011**, 50, 9838–9848.
- (7) For selected examples, see: (a) Gibson, V. C.; Humphries, M. J.; Tellmann, K. P.; Wass, D. F.; White, A. J. P.; Williams, D. J. *Chem. Commun.* **2001**, 2252–2253. (b) Kooistra, T. M.; Knijnenburg, Q.; Smits, J. M. M.; Horton, A. D.; Budzelaar, P. H. M.; Gal, A. W. *Angew. Chem., Int. Ed.* **2001**, 40, 4719–4722. (c) Reardon, D.; Aharonian, G.; Gambarotta, S.; Yap, G. P. A. *Organometallics* **2002**, 21, 786–788. (d) Archer, A. M.; Bouwkamp, M. W.; Cortez, M.-P.; Lobkovsky, E.; Chirik, P. J. *Organometallics* **2006**, 25, 4269–4278. (e) Scott, J.; Vidyaratne, I.; Korobkov, I.; Gambarotta, S.; Budzelaar, P. H. M. *Inorg. Chem.* **2008**, 47, 896–911. (f) Fernández, I.; Trovitch, R. J.; Lobkovsky, E.; Chirik, P. J. *Organometallics* **2008**, 27, 109–118. (g) Bowman, A. C.; Milsman, C.; Bill, E.; Lobkovsky, E.; Weyhermüller, T.; Wieghardt, K.; Chirik, P. J. *Inorg. Chem.* **2010**, 49, 6110–6123.
- (8) For selected examples, see: (a) Scarborough, C. C.; Wieghardt, K. *Inorg. Chem.* **2011**, 50, 9773–9793. (b) Chisholm, M. H.; Huffman, J. C.; Rothwell, I. P.; Bradley, P. G.; Kress, N.; Woodruff, W. H. *J. Am. Chem. Soc.* **1981**, 103, 4945–4947. (c) Koo, K.; Hillhouse, G. L. *Organometallics* **1995**, 14, 4421–4423. (d) Lin, B. L.; Clough, C. R.; Hillhouse, G. L. *J. Am. Chem. Soc.* **2002**, 124, 2890–2891.
- (9) (a) Hulley, E. B.; Wolczanski, P. T.; Lobkovsky, E. B. *J. Am. Chem. Soc.* **2011**, 133, 18058–18061. (b) Frazier, B. A.; Wolczanski, P. T.; Lobkovsky, E. B.; Cundari, T. R. *J. Am. Chem. Soc.* **2009**, 131, 3428–3429.
- (10) Wu, J. Y.; Stanzl, B. N.; Ritter, T. *J. Am. Chem. Soc.* **2010**, 132, 13214–13216.
- (11) Trifonov, A. A.; Gudilenkov, I. D.; Larionova, J.; Luna, C.; Fukin, G. K.; Cherkasov, A. V.; Poddelsky, A. I.; Druzhkov, N. O. *Organometallics* **2009**, 28, 6707–6713.
- (12) Stubbert, Peters, and Gray have recently reported a related bis(iminopyridine) ligand having an Me substituent at the imino carbon: Stubbert, B. D.; Peters, J. C.; Gray, H. B. *J. Am. Chem. Soc.* **2011**, 133, 18070–18073.
- (13) (a) Haga, M.; Koizumi, K. *Inorg. Chim. Acta* **1985**, 104, 47–50. (b) Chakraborty, S.; Munshi, P.; Lahiri, G. K. *Polyhedron* **1999**, 18, 1437–1444.
- (14) (a) Chakraborty, B.; Halder, P.; Paine, T. K. *Dalton Trans.* **2011**, 40, 3647–3654. (b) Zhang, Z.-H.; Chen, S.-C.; He, M.-Y.; Li, C.; Chen, Q.; Du, M. *Cryst. Growth Des.* **2011**, 11, 5171–5175.
- (15) (a) Spikes, G. H.; Bill, E.; Weyhermüller, T.; Wieghardt, K. *Angew. Chem., Int. Ed.* **2008**, 47, 2973.
- (16) Mondal, A.; Weyhermüller, T.; Wieghardt, K. *Chem. Commun.* **2009**, 6098–6100.
- (17) The **1b,c** ratio was determined by the *o*-H signal of the pyridine ring (Figure S8). We assume that the relative positions of the *o*-H protons of the pyridine rings remain the same in the **1b,c** mixture as they are in the **2b,c** mixture (compare Figure S7 and Figure S8). This assumption is supported by the relative positions of other signals in the spectra.
- (18) Calculations were performed at the B3LYP/LANL2DZ/6-31G(d,p) level of theory using a development version of Gaussian. See the Supporting Information for full computational details, energetics, and structures.
- (19) Noodleman, L. *J. Chem. Phys.* **1984**, 74, 5737.
- (20) See the Supporting Information for details about the higher energy states computed.
- (21) Neese, F. J. *Phys. Chem. Solids* **2004**, 65, 781–785.